sustainability

MDPI

Article

Machine Learning-Based GPR with LBFGS Kernel Parameters Selection for Optimal Throughput Mining in 5G Wireless Networks

Joseph Isabona [1], Agbotiname Lucky Imoize [2,3,*], Stephen Ojo [4], Dinh-Thuan Do [5] and Cheng-Chi Lee [6,7,*]

1 Department of Physics, Federal University Lokokja, Lokokja 260101, Nigeria
2 Department of Electrical and Electronics Engineering, Faculty of Engineering, University of Lagos, Lagos 100213, Nigeria
3 Department of Electrical Engineering and Information Technology, Institute of Digital Communication, Ruhr University, 44801 Bochum, Germany
4 Department of Electrical and Computer Engineering, College of Engineering, Anderson University, Anderson, SC 29621, USA
5 School of Engineering, University of Mount Union, Alliance, OH 44601, USA
6 Research and Development Center for Physical Education, Health, and Information Technology, Department of Library and Information Science, Fu Jen Catholic University, New Taipei City 24205, Taiwan
7 Department of Computer Science and Information Engineering, Asia University, Taichung City 41354, Taiwan
* Correspondence: aimoize@unilag.edu.ng (A.L.I.); cclee@mail.fju.edu.tw (C.-C.L.)

Abstract: Considering the ever-growing demand for an efficient method of deductive mining and extrapolative analysis of large-scale dimensional datasets, it is very critical to explore advanced machine learning models and algorithms that can reliably meet the demands of modern cellular networks, satisfying computational efficiency and high precision requirements. One non-parametric supervised machine learning model that finds useful applications in cellular networks is the Gaussian process regression (GPR). The GPR model holds a key controlling kernel function whose hyperparameters can be tuned to enhance its supervised predictive learning and adaptive modeling capabilities. In this paper, the limited-memory Broyden–Fletcher–Goldfarb–Shanno (LBFGS) with kernel parameters selection (KPS) algorithm is employed to tune the GPR model kernel hyperparameters rather than using the standard Bayesian optimization (BOP), which is computationally expensive and does not guarantee substantive precision accuracy in the extrapolative analysis of a large-scale dimensional dataset. In particular, the hybrid GPR–LBFGS is exploited for adaptive optimal extrapolative learning and estimation of throughput data obtained from an operational 5G new radio network. The extrapolative learning accuracy of the proposed GPR–LBFGS with the KPS algorithm was analyzed and compared using standard performance metrics such as the mean absolute error, mean percentage error, root mean square error and correlation coefficient. Generally, results revealed that the GPR model combined with the LBFGS kernel hyperparameter selection is superior to the Bayesian hyperparameter selection method. Specifically, at a 25 m distance, the proposed GPR–LBFGS with the KPS method attained 0.16 MAE accuracy in throughput data prediction. In contrast, the other methods attained 46.06 and 53.68 MAE accuracies. Similarly, at 50 m, 75 m, 100 m, and 160 m measurement distances, the proposed method attained 0.24, 0.18, 0.25, and 0.11 MAE accuracies, respectively, in throughput data prediction, while the two standard methods attained 47.46, 49.93, 29.80, 53.92 and 47.61, 52.54, 53.43, 54.97, respectively. Overall, the GPR–LBFGS with the KPS method would find valuable applications in 5G and beyond 5 G wireless communication systems.

Keywords: 5G wireless networks; throughput data; kernel hyperparameters selection; Gaussian process regression; machine learning; Bayesian optimization; LBFGS–KPS algorithm

check for updates

Citation: Isabona, J.; Imoize, A.L.; Ojo, S.; Do, D.-T.; Lee, C.-C. Machine Learning-Based GPR with LBFGS Kernel Parameters Selection for Optimal Throughput Mining in 5G Wireless Networks. *Sustainability* **2023**, *15*, 1678. https://doi.org/10.3390/su15021678

Academic Editor: Manuel Fernandez-Veiga

Received: 10 November 2022
Revised: 12 January 2023
Accepted: 13 January 2023
Published: 15 January 2023

Copyright: © 2023 by the authors. Licensee MDPI, Basel, Switzerland. This article is an open access article distributed under the terms and conditions of the Creative Commons Attribution (CC BY) license (https://creativecommons.org/licenses/by/4.0/).

1. Introduction

The 5th generation broadband network, largely termed 5G new radio [1–3], is the new evolving global wireless network technology. Overall, 5G has been developed as an

enabler of packet-switch communication, including intelligent transportation, industrial automation, tactile internet, and ultra-high user traffic applications [4]. The robust nature of the ultra-high user traffic requirements ranges from massive connectivity, ultra-reliable communication, and enhanced multimedia mobile broadband services [5–7]. Thus, the rising research on real-time 5G network monitoring, status performance analysis, and predictive data mining aim to ensure that subscribers within the networks are satisfied with the service level agreements. Mainly, throughput data mining and prediction analysis are vital to reduce latency issues in time-critical services in 5G networks [5]. For example, throughput data mining plays a leading role in real-time audio-visual and video-streaming applications, such as YouTube, that involve low-delay network protocols. Therefore, throughput data mining and prediction analysis is needed to guarantee and secure both stable quality of experience (QoE) and quality of service (QoS) in the network [8].

The emergence of advanced machine learning algorithms has revolutionized the design and implementation of modern wireless communication systems [9–11]. A subset of artificial intelligence that counts on any form of real-time data, in combination with algorithms to build systems that learn or perform specific tasks, leveraging experimental data, is in the domain of machine learning [12–15]. The last two decades have witnessed a continuous surge in research and practical applications of machine learning tools, algorithms, and models on a global level across different scientific and engineering fields, including industrial sectors [16].

Machine learning-based algorithms and models are becoming more valuable in data-acquisition systems, deductive mining, and extrapolative data analysis [17]. These models can be applied in all facets of big data mining, including data segmentation, labeling, and analytics. Machine learning also remained a top-shelf artificial intelligence-based tool that automates predictive modeling by training algorithms to detect patterns, learning behaviors in datasets and providing findings for informed decision-making. Particularly, machine learning algorithms applied to large data can be explored to study performance drifts of multinational organizations, learn future trends and provide inference and insights for continuous business growth [18].

1.1. Related Work

Numerous supervised machine learning models exist equipped with computationally efficient algorithms for data extrapolative analytics and knowledge deduction. One prominent among them is the Gaussian process regression (GPR) [19–21]. A key controlling function that can be tuned to further enhance the GRP predictive modeling performance is the kernel function. Several authors have adopted different techniques in the existing literature to select the GPR kernel parameters. The goal is to improve its applications, particularly by engaging the Bayesian optimization (BOP) algorithm. The BOP algorithm works by adding a Bayesian process to an iterative optimization model to solve plausible target function problems.

In [22], a combination of BOP and GPR was employed to resolve the observed computational fluid dynamics problem. The results demonstrate that the use of the BOP–GPR method led to imprecise flow simulations. Finally, a GPR model tuned with BOP is employed in [21] for seawater intrusion prediction. Although time-consuming, the output indicates that the GPR method displayed good performance with root mean square errors ranging between 31.42 and 58.30.

In another related study, an optimized GPR model empowered by the BOP algorithm [23] is exploited for the estimation of confirmed and recovered COVID-19 cases in Brazil and India during the recent pandemic. The resultant precision output shows a high performance compared to other procedures also explored in the estimation process. A similar investigation involving the use of GPR for COVID-19 estimation has been reported using data from Nigeria [24].

Extrapolative BOP algorithm with Gaussian process is applied in comparison with artificial neural network ensembles for the analysis of two different complex datasets with

dissimilar characteristic features [25]. Specifically, the authors employed dense NN and dropout NN. The results displayed 1.68 and 2.21 RMSE values. With the GPR model, the authors also displayed a 1.30 RMSE value.

From the analysis, the enhanced Gaussian process achieved the best performance after 100 iterations through its kernel parameters optimization.

An innovative sparse spectrum-based approximation of GPR with BOP is proposed in [26] to solve the sparse estimation problem. The authors noticed that the proposed method produces less epistemological vagueness than the existing standard methods. In a similar vein, the authors in [27–30] adopted a joint GPR–BOP method for financial applications, leveraging parameter space exploration and reinforcement learning.

In [31], the Rprop algorithm, a gradient-based optimization method, was explored in combination with the GPR model for practical extrapolative analysis. The outcome shows that the GPR–Rprop method provides a consistent optimal solution. A renowned problem with applying the GPR–BOP method is large time consumption and poor precision accuracy on large-scale dimensional datasets [32,33]. In our previous work in [19], a stepwise approach to select optimal kernel based on GPR was proposed to adaptively learn mean throughput quality datasets obtained from operational long-term evolution networks (LTE) [34–36].

In [37], deep learning models have been engaged to predict future network throughput, such as 5G. The result reveals that throughput prediction can be explored as a means of latency reduction in active online streaming services.

In [38], a deep neural network based on the long short-term memory (LSTM) method was employed for 5G network throughput data prediction. The results revealed high root mean square values between 2.23 and 1908.86. A similar deep learning method based on smoothed long short-term memory (SLSTM) is presented by Gao [39] for 5G traffic prediction. A high root mean square error value of 3014.2 was attained by the authors.

In [40], 5G channel stability prediction, in connection with throughput and data loss, was investigated using neural network (NN) and support vector machines (SVM) methods. The authors recorded 96.43% and 92.86% prediction accuracies.

Throughput data prediction with machine learning for LTE and 5G Networks is investigated in [41]. The authors attained 93% and 84% prediction accuracies.

1.2. Contributions

The current paper proposes the application of the limited-memory Broyden–Fletcher–Goldfarb–Shanno (LBFGS) algorithm [42] for GPR kernel hyperparameters optimization [19]. The goal is to attain optimal predictive estimation of highly stochastic 5G throughput data. In particular, the main contributions of the current study are outlined as follows.

- A detailed status analysis of the acquired throughput quality levels attained at different measurements from the transmitter using a unique Gaussian mixture distribution clustering approach is provided.
- The work proposes and shows how the LBFGS with KPS algorithm can be efficiently explored to determine the GPR hyperparameters for enhanced predictive modeling.
- The work quantified and revealed the effectiveness of the proposed hybrid GPR–LBFGS with the KPS method on real-time extrapolative analysis of practical throughput data obtained at different transmitter–receiver communication distances.
- The work provides detailed results showing how the LBFGS with KPS algorithm outperforms the standard Bayesian hyperparameter tuning method using different key performance indexes.
- The current work demonstrates throughput quality enhancement at the user equipment terminals in 5G wireless networks.
- The work provides the implication of the projected results for future wireless communication systems in the beyond-5G era.

1.3. Organization

The remaining part of this paper is organized as follows. Section 2 presents the proposed machine learning-based models. Here, the Gaussian process regression model is introduced. In addition, the squared exponential kernel (SEK) and the optimization of the kernel parameters are briefed. Section 2 also captures the proposed GPR model combined with the LBFGS kernel parameters selection. Section 3 provides a brief description of the 5G throughput measurements. Finally, Section 4 dwells on the key results and useful discussions. The key results comprise throughput quality characterization, throughput adaptive learning, training and testing, performance assessment of the proposed GPR–LBFGS with KPS algorithm, and the measured 5G throughput quality performance and implication for beyond-5G wireless networks. Summarily, Section 5 concludes the paper and provides future perspectives.

2. The Proposed Machine Learning-Based Model

We provide detailed information on the proposed machine learning-based model in this paper, which is the Gaussian process regression model. The squared exponential kernel is considered, followed by the optimization of the kernel parameters. Furthermore, the proposed GPR model with limited-memory Broyden–Fletcher–Goldfarb–Shanno (LBFGS) kernel parameters selection algorithm is broached. The LBFGS with the KPS algorithm is presented next. Lastly, we highlight the GPR model with the proposed LBFGS kernel parameters selection algorithm.

2.1. Gaussian Process Regression Model

A Gaussian process regression (GPR) model is a non-parametric predictive learning model which makes use of the covariance function and its mean. Thus, a GPR can be wholly defined by the covariance function and its mean [43–45].

Given a throughput dataset, Ω_{train}= $[(x_i, y_i)]_{i=1}^{n}$, for training, with x_i and y_i defining the input and target variable quantities. The model function $f(x)$ that connects x_i and y_i can be expressed in (1) [19]:

$$y_i = (f(x_i) + \zeta_i; i = 1, 2, \ldots, n) \tag{1}$$

where $\zeta_i = N(0, \sigma_i^2)$ indicates the mean noise model with σ_i^2 being the variance.

In GPR, it is assumed that the $f(x)$ follows a distributed Gaussian process. The observed target can be equally defined using Equation (2):

$$(x_i) \approx GP(m(x_i), K(X, X')); i = 1, 2, \ldots, n \tag{2}$$

with $K(X, X')$ articulating the covariance matrix and $m(x_i) = E[f(x_i)]$ being an expectation function for input, x_i.

The GPR prediction output component of the input vector expressions in (1) and (2) can be described as (3) with its parameters defined in (4)–(7):

$$\begin{vmatrix} \vec{y} \\ \vec{f'} \end{vmatrix} X, X' \approx N\left(\vec{0}, \begin{bmatrix} K(\mathrm{X}, \mathrm{X}) + \sigma_i^2 \mathrm{I}\, \mathrm{K}(\mathrm{X}, \mathrm{X}') \\ \mathrm{K}(\mathrm{X}', \mathrm{X})\ \mathrm{K}(\mathrm{X}', \mathrm{X}') \end{bmatrix}\right) \tag{3}$$

where

$$X = \begin{bmatrix} -(x_1)T \\ -(x_2)T \\ \vdots \\ -(x_k)T \end{bmatrix} \epsilon \mathrm{R}^{\mathrm{nxm}}, \ \vec{y} = \begin{bmatrix} (y_1)T \\ (y_2)T \\ \vdots \\ (y_k)T \end{bmatrix} \epsilon\ \mathrm{R}^{\mathrm{m}} \tag{4}$$

$$\vec{y} = \begin{bmatrix} f(x_1)T \\ f(x_2)T \\ \vdots \\ f(x_k)T \end{bmatrix} \epsilon \, \mathrm{R}^{\mathrm{mxn}}, \; \epsilon = \begin{bmatrix} (\epsilon_1) \\ (\epsilon_2) \\ \vdots \\ (\epsilon_k) \end{bmatrix} \epsilon \, \mathrm{R}^{\mathrm{m}} \tag{5}$$

$$X' = \begin{bmatrix} -(x_1)T \\ -(x_2)T \\ \vdots \\ -(x_k)T \end{bmatrix} \epsilon \, \mathrm{R}^{\mathrm{nxm}}, \; \vec{y}' = \begin{bmatrix} (y_1')T \\ (y_2')T \\ \vdots \\ (y_k')T \end{bmatrix} \epsilon \, \mathrm{R}^{\mathrm{m}'} \tag{6}$$

$$\vec{f}' = \begin{bmatrix} f(x_1')T \\ f(x_2')T \\ \vdots \\ f(x_k')T \end{bmatrix} \epsilon \, \mathrm{R}^{\mathrm{m}' \, \mathrm{n}}, \; \epsilon = \begin{bmatrix} (\epsilon_1') \\ (\epsilon_2') \\ \vdots \\ (\epsilon_k') \end{bmatrix} \epsilon \, \mathrm{R}^{\mathrm{m}'} \tag{7}$$

and $K(\mathrm{X}, \mathrm{X}) \, \epsilon \, \mathrm{R}^{\mathrm{mx\,n}}$, $K(\mathrm{X}, \mathrm{X}') \, \epsilon \, \mathrm{R}^{\mathrm{mx\,n}'}$, $K(\mathrm{X}', \mathrm{X}) \, \epsilon \, \mathrm{R}^{\mathrm{m}'\,\mathrm{n}}$ and $K(\mathrm{X}', \mathrm{X}') \, \epsilon \, \mathrm{R}^{\mathrm{m}'\mathrm{x}\,\mathrm{n}'}$.

2.2. Squared Exponential Kernel

Several kernel GPR-based kernel functions exist in the literature, but the one in focus here is the squared exponential kernel (SEK) [46]. SEK is the most extensively utilized kernel owing to its moderate robustness and precision. It also guarantees a productive and positive covariance irrespective of input data dimensions. However, SEK optimal performance is dependent on the numerical reliability condition of the kernel matrix. For example, they possess two hypermeters, namely the characteristic length scale (ls) and the noise signal (Sn). A large ls value will map the narrower range of input values, whereas a small ls value will result in the opposite. Accordingly, a large ls indicates long-range output correlations. In contrast, a short ls will make the input strongly map the target output values, but on the condition that the respective inputs are very closely correlated.

2.3. Optimizing Kernel Parameters

Every kernel function has its own key parameter sets, such as signal variance, length scale, and noise variance, that are usually unknown and have to be deduced directly from the observed data. In GPR, since these key parameters greatly influence the target function resources, they are called the hyperparameters of the GPR model.

A standard method for estimating or obtaining these hyperparameters is maximizing the marginal (log) likelihood. This is known as the likelihood parameter estimation method [47]. Given the data, $\Omega_{train} = [(x_i, y_i)]_{i=1}^{n}$ and hyperparameters θ, such that $\theta = (\lambda, \sigma^2)$, the log marginal likelihood is given in (8):

$$logp(y/X, \theta) = -\frac{1}{2} y^T K_y^{-1} - \frac{1}{2} log/K_y/ - \frac{n}{2} log 2\pi \tag{8}$$

where $K_y = K(\mathrm{X}, \mathrm{X}) + \sigma_i^2 \mathrm{I}$ expresses the covariance matrix. Equation (9) is obtained by taking the partial derivatives of the expression in (8) with respect to θ.

$$\frac{\partial logp(y/X, \theta)}{\partial \theta_j} = -\frac{1}{2} y^T K_y^{-1} - \frac{1}{2} tr\left(K_y^{-1} \frac{\partial (Ky)}{\partial \theta_j} \right) = -\frac{1}{2} tr\left(K_y^{-1} K_y^{-T} - K_y^{-1} \frac{\partial (K_y)}{\partial \theta_j} \right) \tag{9}$$

Another known standard method to determine the kernel hyperparameters is the Bayesian optimization [21,22,48]. However, a key problem with the approach is its poor performance accuracy on large-scale dimensional and noisy data [19,49,50]. It also wastes time and scales poorly when many hyperparameters are involved in tuning.

2.4. Proposed GPR Model with LBFGS Kernel Parameters Selection

The methodology employed is an expository stepwise approach described as follows. The parameters selection commenced by providing background information on the Gaussian process, leveraging the theoretical framework and the relevance of its kernel hyperparameter selection. This is followed by presenting the proposed kernel hyperparameter selection. The highlight of how the GPR model with the proposed LBFGS kernel parameters selection algorithm is provided as follows:

1. Load the throughput datasets into the MATLAB workspace.

```
load('data');
Throughput [Mbps]= [ ]';
Data_point = [ ]';
```

2. Engage the GMM model to examine the entire throughput dataset characteristics at the different acquisition distances.

```
k = 3; % Number of GMM components
options = statset('MaxIter', 1000);
Sigma = {'diagonal','full'}; % Options for covariance matrix type
d = 500; % Grid length
% Call the GMM fit in MATLAB format
gmfit = fitgmdist()
```

3. Eliminate the missing values/outliers and standardize the outputs/input predictors.

```
% Call the outlier/standardization encryption
B = rmoutliers(A);
N = normalize(B, method)
```

4. Divide the throughput datasets into two with 0.7 components for training and 0.3 component for testing.

```
% Use 70% to training set + 30% to testing set and cross-validation (train: 70%, test: 30%)
PD = 0.30; % percentage 30%
cv = cvpartition(size(data,1),'HoldOut',PD);
idx = cv.test;
% Separate to training and test data
dataTrain = data(~idx,:);
X_train = dataTrain(:,1:end-1); Y_train = dataTrain(:,end);
X = X_train; y = Y_train;
```

5. Explore the GPR prediction model with default kernel parameters for throughput datasets training/testing

```
gprMdl = fitrgp(x,y,'Basis','linear',...
'FitMethod','exact','PredictMethod','exact');
Examine the kernel information using gprMdl.KernelInformation
```

6. Appraise the resultant outcome of step (e) above and save the results.

```
error = y-ypred; ms_error = mse(y-ypred)
MAE = mae(y-ypred); RMSE = sqrt(ms_error);
```

7. Engage the GPR prediction model with the proposed LBFGS kernel parameters selection algorithm for throughput datasets training/testing.

```
% Call in the GPR function (gprMdl1) with the proposed LBFGS optimizer and the square exponential function (kfcn) with distance matrix, pdist2 (XN,XM).^2
gprMdl1 = fitrgp ( )
kfcn = @(XN,XM,theta) (exp(theta (2))^2)*exp(-(pdist2(XN,XM).^2)/(2*exp(theta(1))^2));
```

8. Appraise the resultant outcome of step (g) above and save the results.

```
error = y-ypred; ms_error = mse(y-ypred)
```

MAE = mae(y-ypred); RMSE = sqrt(ms_error);

9. Compare the results from step (h) with the results of (f) and the outcome of other standard methods.
10. If the resultant outcome is satisfactory, stop; otherwise, go through steps (f) to (i).

These steps are summarized as shown in Figure 1, emphasizing machine learning based on GPR with LBFGS kernel parameters selection.

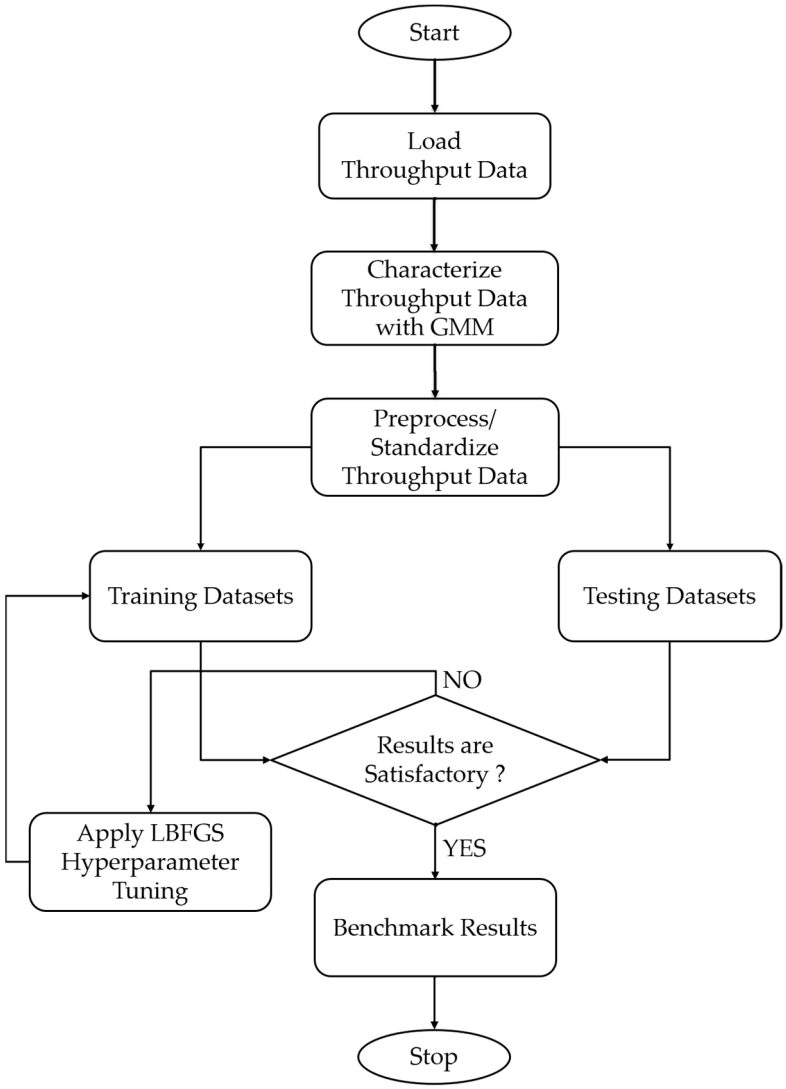


Figure 1. Machine learning based on GPR with LBFGS kernel parameters selection algorithm.

2.5. The LBFGS Algorithm

The LBFGS algorithm established by Liu and Nocedal in 1989 [51] is a fast and efficient numerical-based optimization algorithm for solving various large-scale problems, particularly within the domain of the artificial network. The LBFGS is an optimized version of the BFGS technique, and its memory requirement is about $(12 + 2m)N$, where N and m indicate the model space size and BFGS update number, respectively [52,53]. The LBFGS achieves its adaptive optimization by employing inverse Hessian matrix approximation [54,55] via iterative processes to pilot its line search over variable space as given in (10)–(15):

$$\theta_{t+1} = \theta_t - \alpha_t H_t \Delta f(\theta_t) \quad (10)$$

$$H_{t+1} = V_t^T H_t V_t + q_t \, s_t^T s_t \, \frac{H_t \, K_t^T}{q_t^T s_t} \tag{11}$$

$$s_t = \theta_{t+1} - \theta_t \tag{12}$$

$$q_t = \Delta f(\theta_{t+1}) - \Delta f(\theta_t) \tag{13}$$

$$q_t \; = \frac{1}{q_t^T s_t} \tag{14}$$

$$V_t V_t^T = 1_t + q_t \, s_t^T s_t \tag{15}$$

The LBFGS update is iteratively generated sequentially until a convergence termination condition is satisfied and improved approximate solutions for θ are reached. At every iteration t as defined in Equation (10), the LBFGS approaches the function $f(\theta_t)$ and computes the H_t at the point θ_t and α_t indicates the learning rate (or step length) that regulates each iteration step size. The LBFGS implementation step is given as:

1. Procedure LBFGS
2. Select the input starting point θ_0, α_0
3. $t \leftarrow 0$
4. While true, do
5. Compute $H_t \Delta f(\theta_t)$ at θ_t current point
6. Compute the change in θ via the expression in (10):
7. $\theta_{t+1} = \theta_t - \alpha_t H_t \Delta f(\theta_t)$
8. end if
9. Calculate and save $s_t = \theta_{t+1} - \theta_t$ and $q_t = \Delta f(\theta_{t+1}) - \Delta f(\theta_t)$
10. $t \leftarrow t + 1$
11. End while
12. End procedure until convergence

3. Description of 5G Throughput Measurements

The telecommunications industry is one of the key sectors undergoing rapid and continuous evolution of different multimedia and cellular-based broadband communication technologies, such as high-speed packet access (HSPA) [56], long-term evolution (LTE) [57,58], new radio (NR) [2,59,60], among others. Continuous measurement-based data facilitate monitoring, performance evaluation, and optimization of the wireless network [35,61–63]. Data collection and mining are crucial for performance monitoring and event-driven decision making from the design phase to the operational cycle of a typical telecommunication system. Furthermore, AI-based algorithms need robust data for effective predictive learning and analytics processes. In the current study, throughput, which measures the number of packets that reach their destinations, is measured and analyzed.

In the current study, extensive throughput measurements collected by researchers from several urban environments of Minneapolis in the United States were used to analyze, test, and validate the projected machine learning-based models. Specifically, the field measurements, which are available online [64], were taken using two 5G smartphones (Motorola Moto Z3 and Samsung Galaxy S10 5G (SM-G977U)). The goal of the extensive measurement is to examine the performance of operational 5G wireless networks on smart mobile devices. Specifically, the researchers investigated the 5G networks of three popular carriers in three large cities in the United States. Among the tested parameters are handoff mechanisms in the 5G network and how these handoff mechanisms impact the performance of the network.

The authors also assessed how various apps performed over the tested 5G wireless networks during web browsing, online downloading, and video streaming. In particular, 15Tb data were used for the extensive experiments via Verizon, T-Mobile, and Sprint 5G networks. It is worth mentioning that the Verizon network uses the mmWave 5G services in the tested environments. T-Mobile also employs the mmWave band, and Sprint operates

at 2.5 GHz. The measurements were carried out against a Microsoft Azure server to obtain a very high 5G throughput of up to 3 Gbps [50].

In addition to throughput quality, the other key quality parameter measured at distances during the field test is the round trip delay (RTD) [65]. The RTD expresses the amount of time (duration) it takes a sender (i.e., subscriber) to send information (message) through a communication channel and receive a feedback response. This paper concentrates on 5000 throughput data collected spatially and at different time sequences.

Lastly, the scripts and graphical results presented in this study were realized in the MATLAB environment installed on an HP laptop (Elitebook). The Elitebook possesses an Intel® Core™ i5-10110U with 4 MB-L3-cache computation-busting technology.

4. Results and Discussion

The results and useful discussions are presented in this section. First, the results of throughput quality characterization are presented. Next, the results of throughput adaptive learning, including training and testing, are highlighted. Additionally, the performance assessment of the proposed approach is demonstrated. Lastly, the implication of the measured 5G throughput quality performance for beyond-5G wireless networks is discussed briefly.

4.1. Throughput Quality Characterization

The Gaussian mixture model (GMM) [33], which is a unique distribution-clustering-based modeling algorithm, was used to provide a detailed description of the practical throughput quality data characteristics obtained at different measurement distances (25, 50, 75, 100, and 160 m). The GMM clustering approach assembles throughput quality levels with similar correlation sizes and their constituent characteristics, as displayed in Figures 2–5. Specifically, Figure 2 gives the measured throughput characterization at 25 m as a function of different measurement points with time. Figure 3 provides the measured throughput characterization at 50 m. Figure 4 shows the measured throughput characterization at 75 m. Figure 5 depicts the measured throughput characterization at 100 m. Lastly, Figure 6 elaborates on the measured throughput characterization at 160 m.

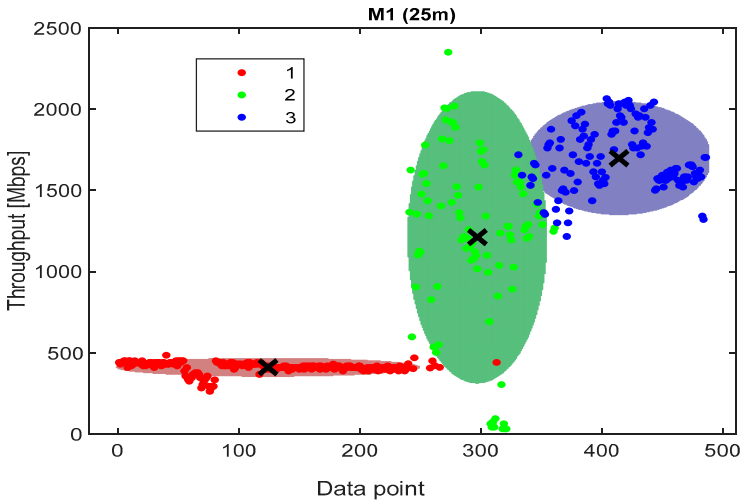


Figure 2. Measured throughput characterization at 25 m.

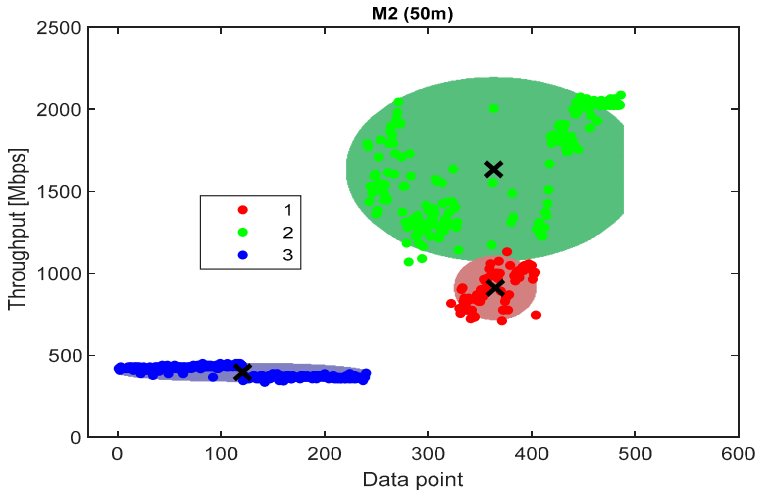


Figure 3. Measured throughput characterization at 50 m.

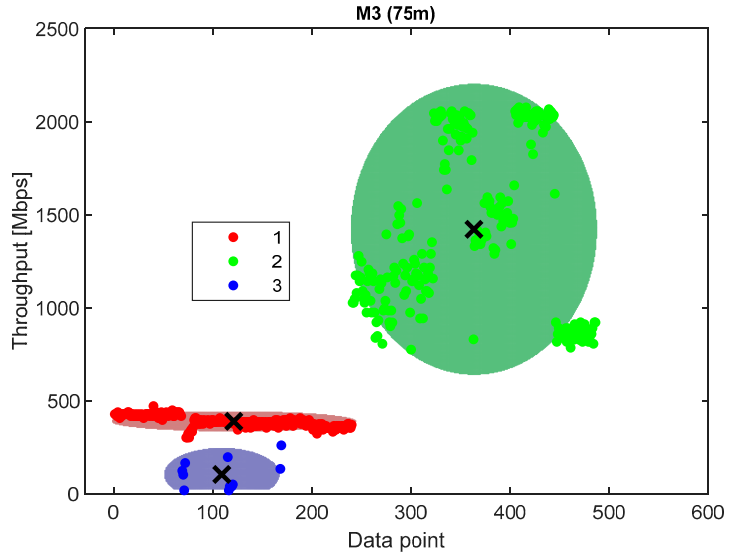


Figure 4. Measured throughput characterization at 75 m.

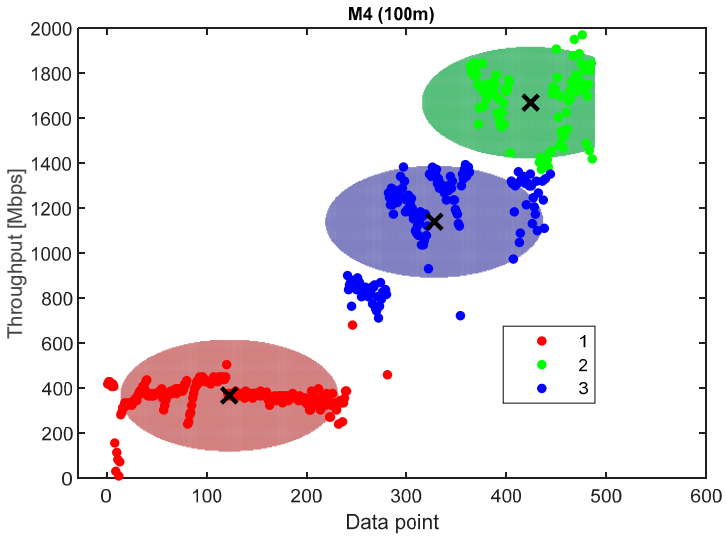


Figure 5. Measured throughput characterization at 100 m.

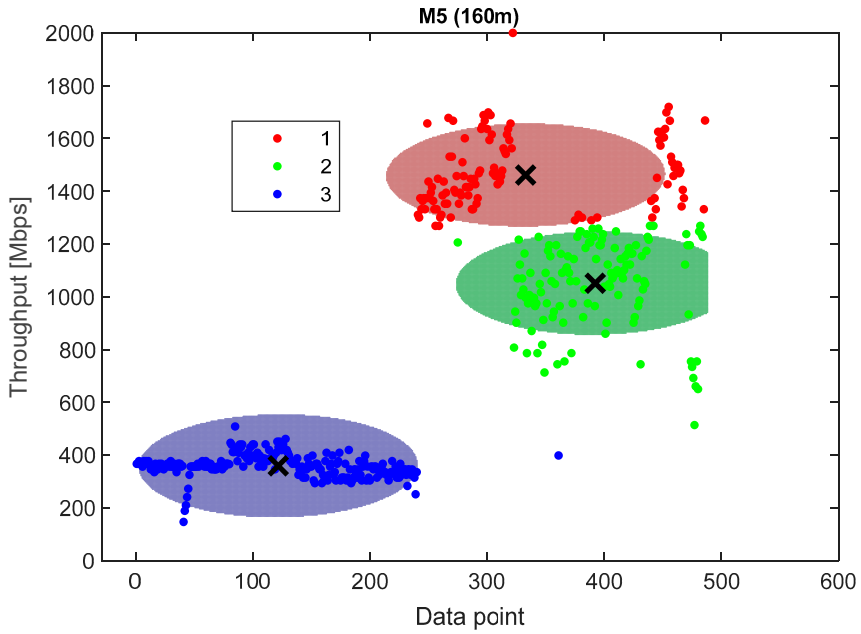


Figure 6. Measured throughput characterization at 160 m.

In Figure 2, the first cluster distribution contour in red indicates that 5G networks provide relatively flat and low throughput quality levels between 31–400 Mbps at the initial stage of the user equipment login. The flat but low throughput quality performance may be due to pick-up issues, network delay, and packet retransmission problems. The second cluster in green color reveals the upward-rising performance of the throughput quality as the spatial measurement is continuous. This implies that the acquired spatial throughput quality data change with time after the initial login by the user. In Figure 2, this occurred for throughput above 430 Mbps. The last third cluster reveals a relatively fluctuating stable quality attained as the measurement proceeds, and this is observed at 320 Mpbs and above. A close look at the results reveals that the throughput values were also relatively stable between 1500 and 2024 Mbps. The same throughput quality performance trends can be seen in the results shown in Figures 3, 5 and 6, but not in Figure 4. The general throughput quality fluctuations at different measurement points can be ascribed to different factors, such as bandwidth congestion, partial network failures, propagation channel bottlenecks, retransmission problems, long- and short-term fading issues, and different environmental and man-made impediments.

4.2. Throughput Adaptive Learning: Training and Testing

When delivering different packet-switch services and applications to users, throughput quality remained a key quality parameter that can be explored to examine operational network performance status and the level of user satisfaction. It also provides good means of proactively detecting and diagnosing the rate of packet data transmission quality issues in the network. Particularly, throughput data mining and prediction analysis are vital to latency issues' reduction in time-critical services in 5G networks. Throughput data mining plays a leading role in real-time audio-visual and video-streaming applications, such as YouTube, that involve low-delay network protocols. By throughput we mean the quantity of data in packets that arrived successfully at their intended destinations within a given timeframe after being transferred from source through the communication channel and which can be transferred from source to destination.

Here, in order to apply the GPR model with the proposed LBFGS with the KPS algorithm (KPS algorithm for brevity) for adaptive learning, the acquired throughput datasets were divided into two using a 70:30% ratio: 70% for the model training and the remaining 30% for testing. Figures 7–11 are the prediction training and testing results.

In particular, Figure 7 shows the predicted throughput data at 25 m measurement with the proposed LBFGS with the KPS method and other standard methods. Figure 8 shows the predicted throughput data at 50 m measurement with the proposed LBFGS with the KPS method and other standard methods. Figure 9 depicts the predicted throughput data at 75 m measurement with the proposed LBFGS with KPS method and other standard methods. Figure 10 presents the predicted throughput data at 100 m with the proposed LBFGS with KPS and other standard methods. Figure 11 captures the predicted throughput data at 160 m measurement with the proposed LBFGS with the KPS method and other standard methods. Also presented in each of Figures 7–11 are the prediction performances achieved with the GPR model tuned by the Bayesian optimization algorithm and the standard GPR models with default parameters.

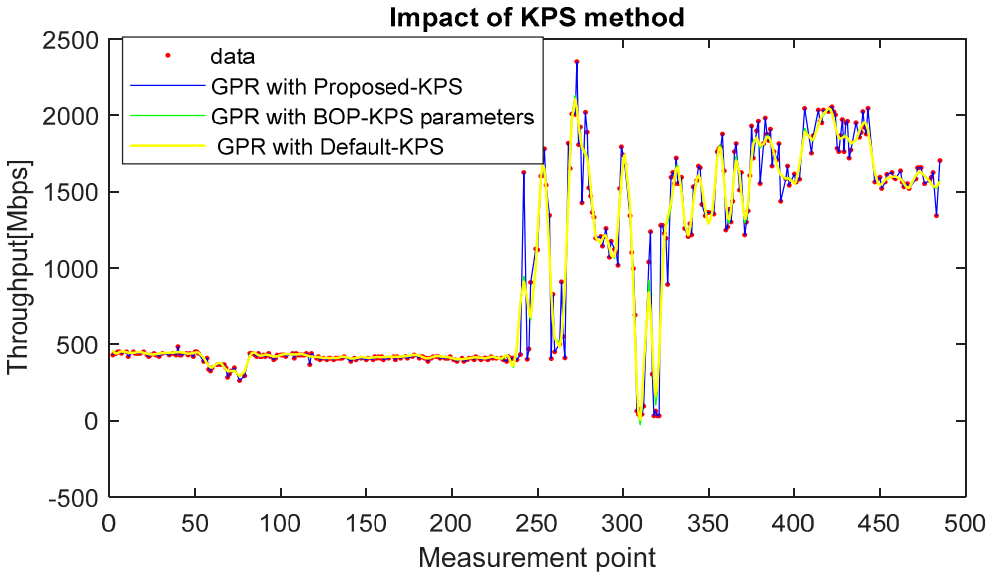


Figure 7. Predicted throughput data at 25 m measurement with proposed LBFGS with KPS method and other standard methods.

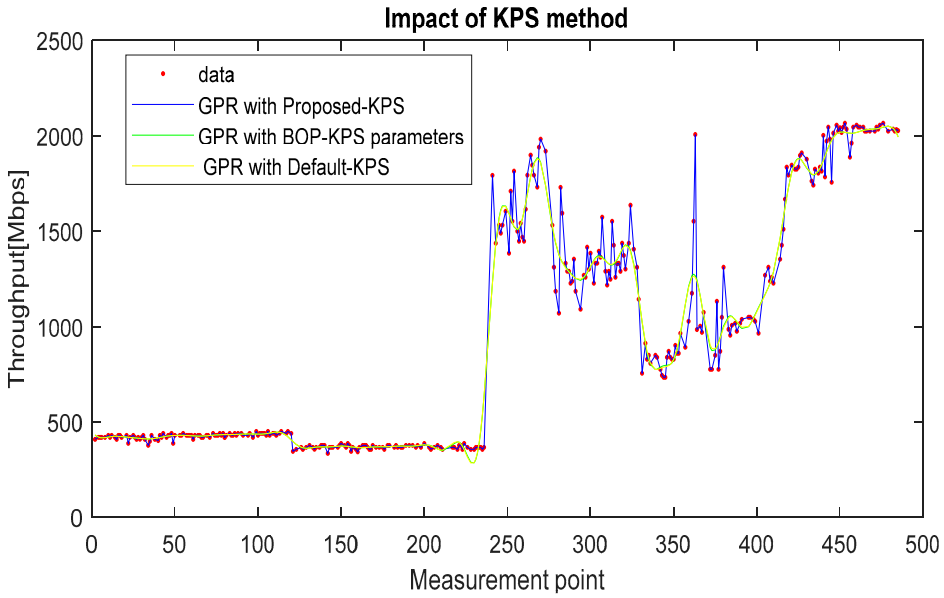


Figure 8. Predicted throughput data at 50 m measurement with proposed LBFGS with KPS method and other standard methods.

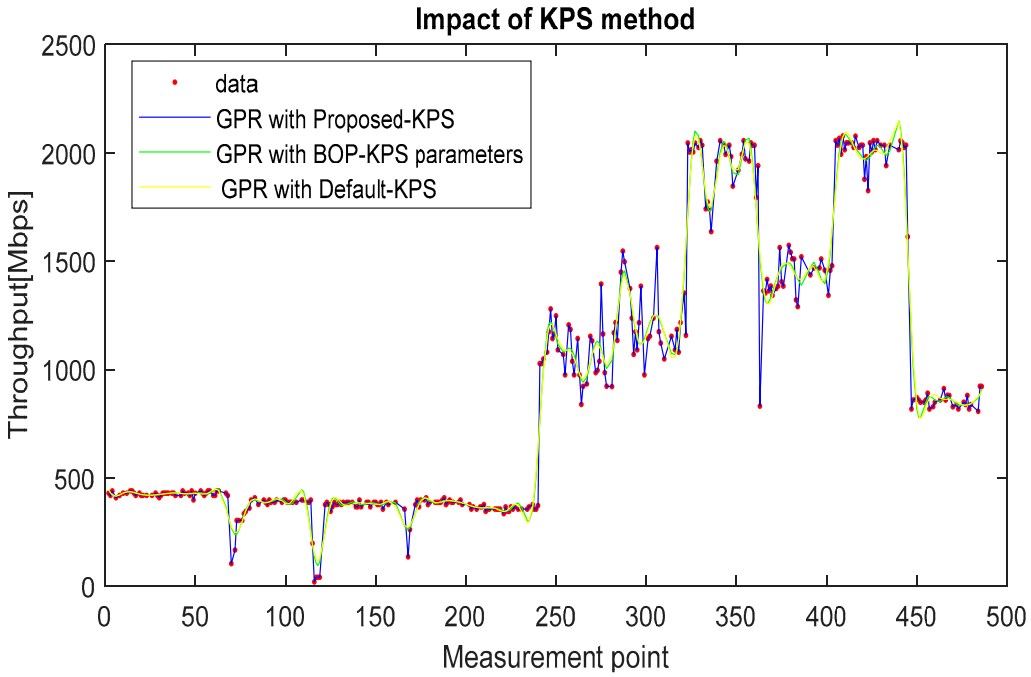


Figure 9. Predicted throughput data at 75 m measurement with proposed LBFGS with KPS method and other standard methods.

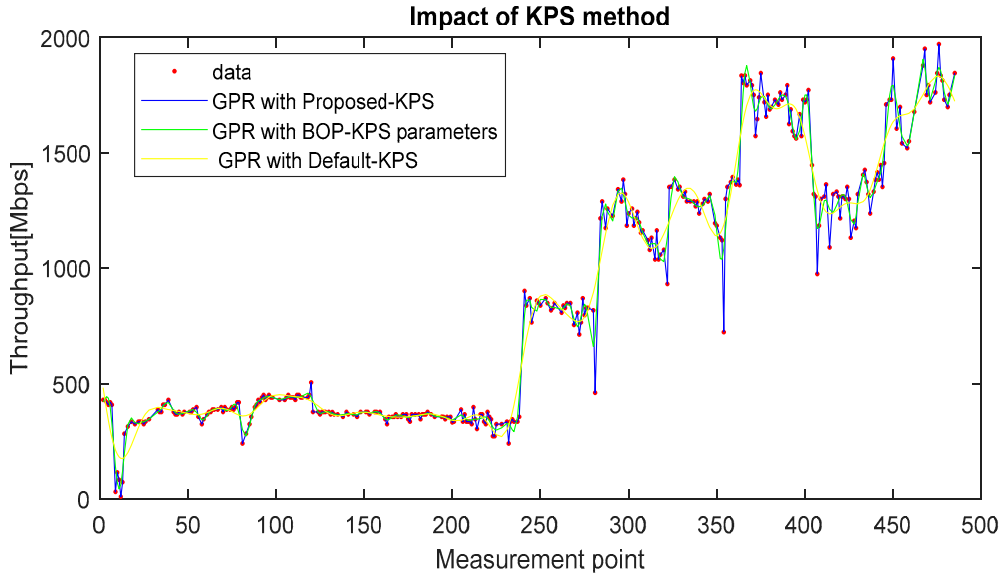


Figure 10. Predicted throughput data at 100 m measurement with proposed LBFGS with KPS method and other standard methods.

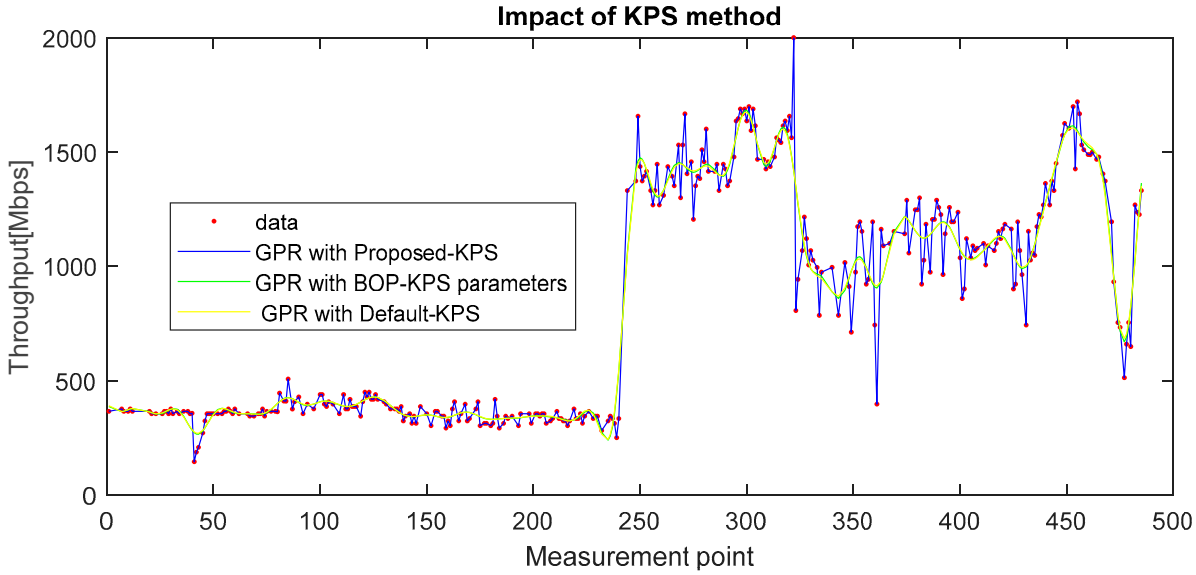


Figure 11. Predicted throughput data at 160 m measurement with proposed LBFGS with KPS method and other standard methods.

Overall, ten GPR kernel functions were investigated and their predictive learning performances were assessed rigorously. During the learning process, the RMSEs obtained are as shown in the data points of the plots presented. The normalized distribution curves were fitted to examine performance. It is worth mentioning that the frequency distributions agree closely with the measured physical downlink shared channel (PDSCH) throughput and the kernel-controlled GPR model at all tested data points.

The GPR standard approach with default parameters and the one trained with Bayesian optimization performed the poorest on the predicted throughput. GPR generally does not scale-fit poorly to high-dimensional data and observations with many variables [19].

4.3. Performance Assessment of the Proposed GPR–LBFGS with the KPS Algorithm

Five goodness-of-fit statistical measures comprising the root mean error (RMSE), correlation coefficient (R), mean absolute error (MAE), standard deviation (STD), and mean percentage error (MAPE) were considered for testing the superiority of the proposed model over other methods [66]. The RMSE defines the degree of the square error averages between the difference between the predicted throughput and the actual observed values. MAE expresses the magnitude of mean absolute error differences between the predicted throughput values and the actual observed values. The coefficient of determination, R, indicates how the predicted throughput values correlate with the actual observed values. STD expresses the amount by which the predicted throughput values deviate from the real values. Thus, a higher STD value indicates the predicted throughput values diverge largely from the actual observed values. Except for R, the lower the RMSE, MAPE, MAE, and STD values indicated, the better the prediction process is.

Generally, results show that the proposed GPR model with the LBFGS–KPS algorithm outperforms other methods due to its ability to iteratively provide better estimates of the kernel parameters during the optimization process, as shown in Figures 12–16. In particular, Figure 12 depicts the predicted and measured throughput correlation performance at 25 m using: (A) GPR with the proposed LBFGS with the KPS method, (B) GPR with the BOP–KPS method, and (C) GPR with default parameters. Figure 13 provides the predicted and measured throughput correlation performance at 50 m using: (A) GPR with the proposed KPS method, (B) GPR with the BOP–KPS method, and (C) GPR with default parameters. Figure 14 shows the predicted and measured throughput correlation performance at 75 m

using: (A) GPR with the proposed LBFGS with the KPS method, (B) GPR with the BOP–KPS method, and (C) GPR with default parameters. Figure 15 provides the predicted and Measured throughput correlation performance at 100 m using: (A) GPR with the proposed LBFGS with the KPS method, (B) GPR with the BOP–KPS method, and (C) GPR with default parameters. Figure 16 shows the predicted and measured throughput correlation performance at 160 m using: (A) GPR with the proposed KPS method, (B) GPR with the BOP–KPS method, and (C) GPR with default parameters.

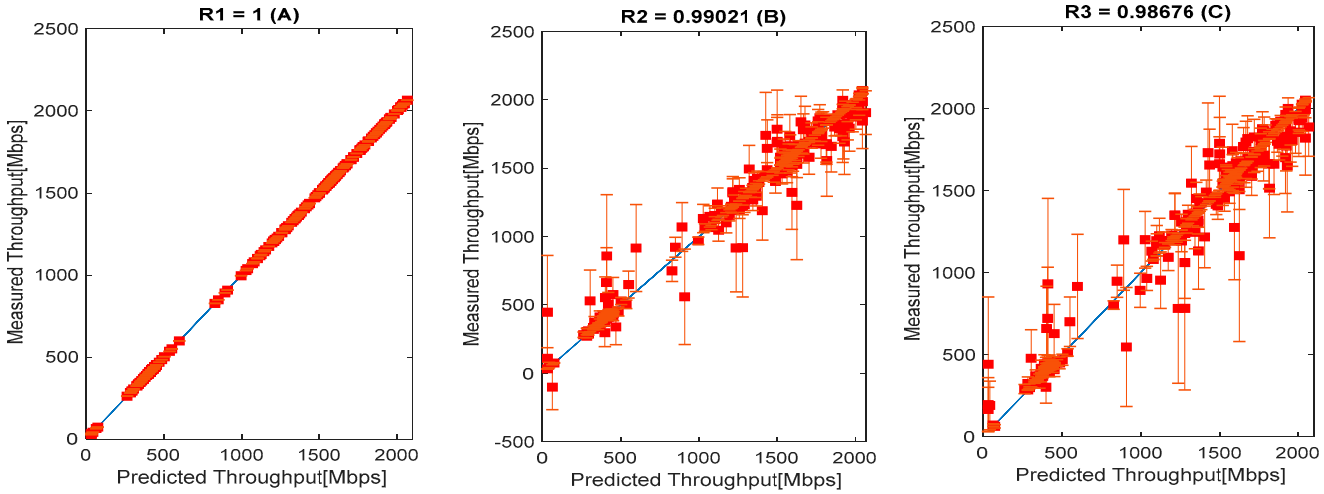


Figure 12. Predicted and measured throughput correlation performance at 25 m using: (**A**) GPR with the proposed LBFGS with the KPS method, (**B**) GPR with the BOP–KPS method, and (**C**) GPR with default parameters.

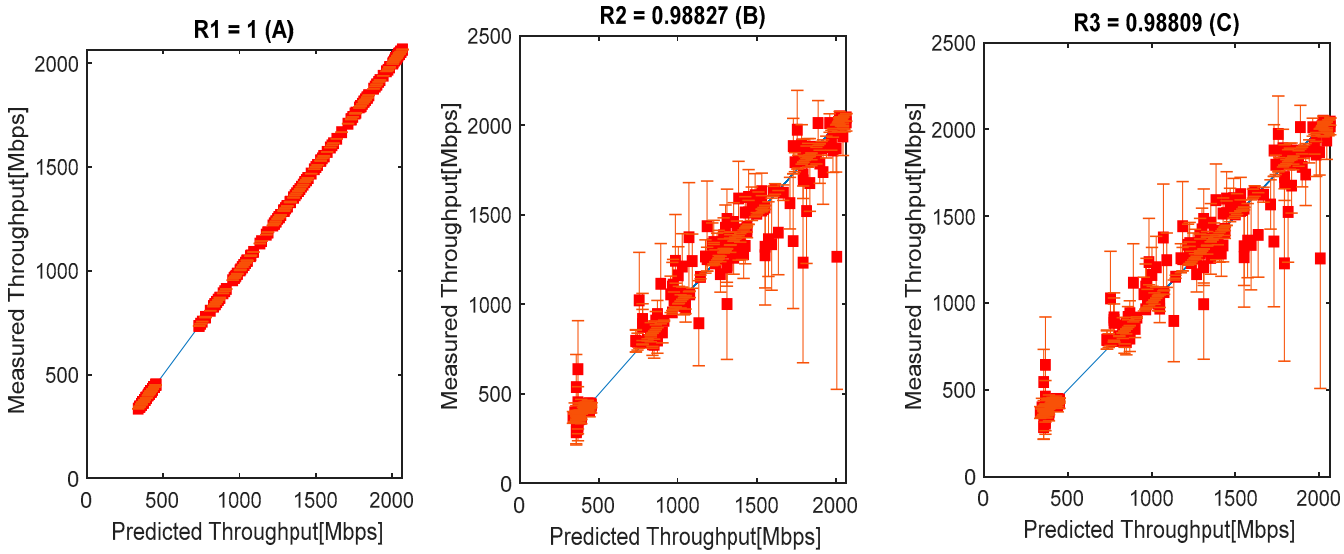


Figure 13. Predicted and measured throughput correlation performance at 50 m using: (**A**) GPR with the proposed LBFGS with the KPS method, (**B**) GPR with the BOP–KPS method, and (**C**) GPR with default parameters.

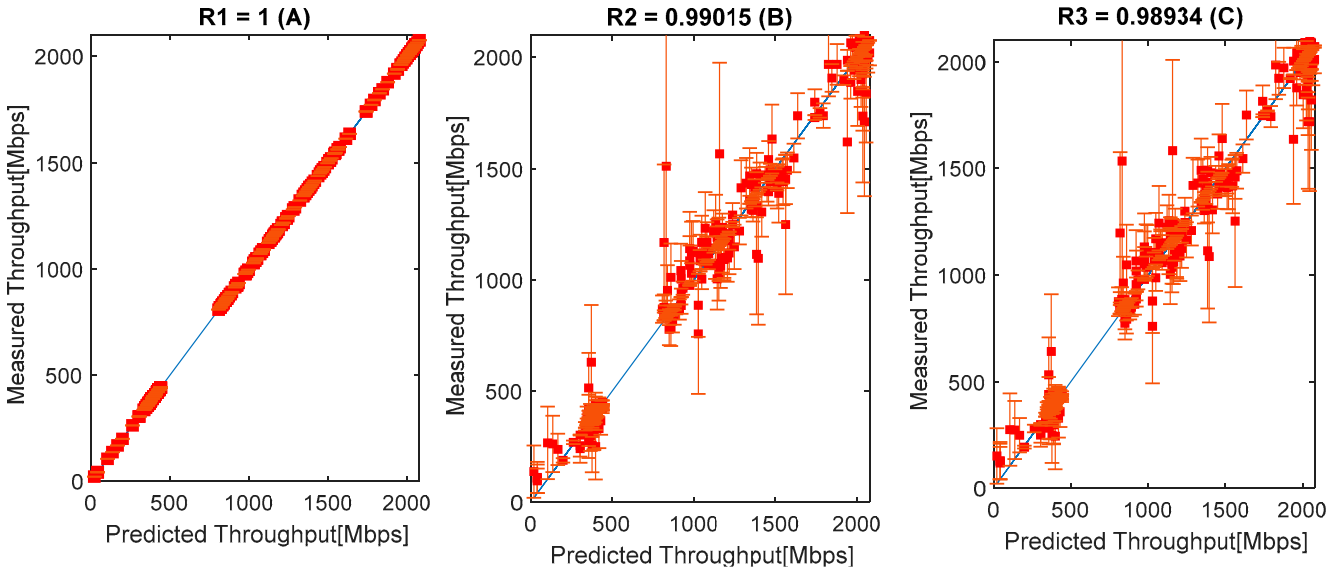


Figure 14. Predicted and measured throughput correlation performance at 75 m using: (**A**) GPR with the proposed LBFGS with the KPS method, (**B**) GPR with the BOP–KPS method, and (**C**) GPR with default parameters.

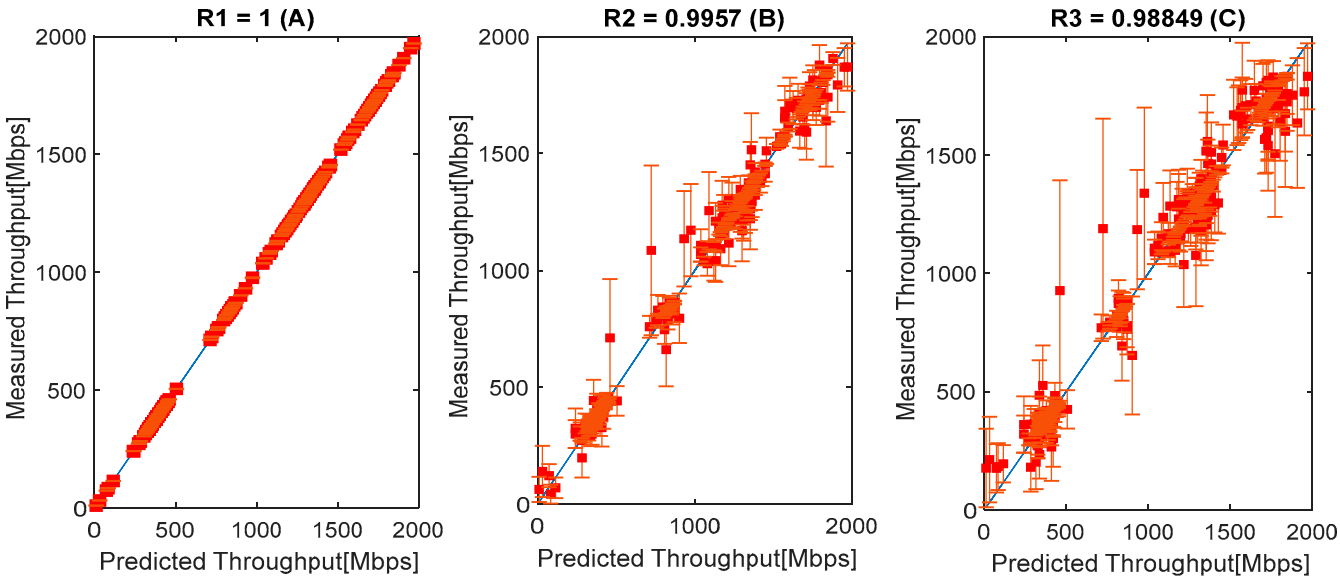


Figure 15. Predicted and measured throughput correlation performance at 100 m using: (**A**) GPR with the proposed LBFGS with the KPS method, (**B**) GPR with the BOP–KPS method, and (**C**) GPR with default parameters.

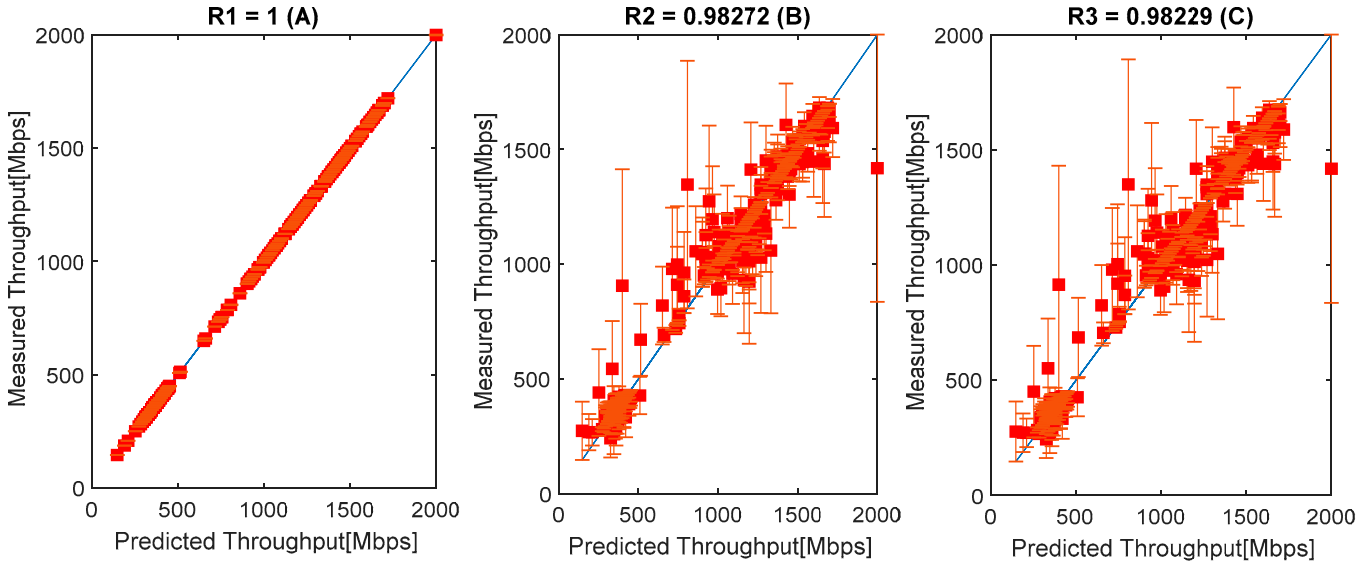


Figure 16. Predicted and measured throughput correlation performance at 160 m using: (**A**) GPR with the proposed LBFGS with the KPS method, (**B**) GPR with the BOP–KPS method, and (**C**) GPR with default parameters.

The optimization involves conducting an enhanced line search of the kernel parameters that best minimize the prediction errors. At a 25 m distance, the proposed method attained 0.25 RMSE value accuracy, while the other methods attained 2.5 and 3 RMSE accuracies. At 50 m, the proposed method attained 0.16 RMSE value accuracy, while the other methods attained 4.3 and 30 RMSE accuracies. At 75 m, the proposed method attained 0.16 RMSE accuracy, while the other methods attained 4.3 and 30 RMSE accuracies. At 100 m, the proposed method attained 0.22 RMSE value accuracy, while the other methods attained 30 and 34 RMSE accuracies. At 160 m, the proposed method attained 0.43 RMSE accuracy, while the other methods attained 4.1 and 20 RMSE value accuracies.

Additionally, Figures 12–16 display the correlation plot performances of the proposed method over other approaches. The superior adaptive predictive learning capacity of the GPR model with the LBFGS combined with the KPS algorithm during training is presented in comparison with the other two standard methods. The superior precision accuracies of adaptive predictive learning capacity are quantified using MAE and R values. At 25 m, the proposed method attained 0.54 of MAE and 0.9651 of R accuracies, while the GPR with the Bayesian optimization algorithm attained 40.41 of MAE and 0.9921 of R accuracies. At 50m, the proposed method attained 6.55 of MAE and 0.9976 R accuracies, while the GPR with the Bayesian optimization algorithm attained 40.4 of MAE and 0.9921 R accuracies.

At 75 m, the proposed method attained 0.41 of MAE and 0.9888 of R accuracies, while the GPR with Bayesian optimization algorithm attained 10.49 of MAE and 0.9940 of R accuracies. At 50m, the proposed method attained 0.41 of MAE and 0.9681 of R accuracies, while the GPR with the Bayesian optimization algorithm attained 43.23 of MAE and 0.9921 of R accuracies. At 160 m, the proposed method attained 0.80 of MAE and 0.9866 of R accuracies, while the GPR with the Bayesian optimization algorithm attained 40.09 of MAE and 0.90867 of R accuracies. Table 1 provides a concise summary of the precision performance of the proposed approach over other existing approaches in terms of MAE, RMSE, MAPE, and STD values.

Table 1. Performance characteristics of the proposed approach over the existing approaches in terms of some standard metrics—MAE, RMSE, MAPE and STD values.

		Training				Testing			
Dist. (m)	**Method**	**RMSE**	**MAE**	**MAPE**	**STD**	**RMSE**	**MAE**	**MAPE**	**STD**
25	P-KPS	0.35	0.16	0.08	0.31	0.48	0.16	0.04	0.46
	BOP-KPS	86.69	46.06	4.44	73.44	124.72	70.18	1.39	103.10
	D-KPS	101.01	53.68	6.09	85.56	312	178.07	19.19	257.16
50	P-KPS	0.55	0.24	0.02	0.49	0.28	0.11	0.01	0.25
	BOP-KPS	92.31	47.46	4.75	79.18	124.77	69.60	6.97	103.55
	D-KPS	93.03	47.61	4.77	79.92	124.56	69.41	6.96	103.36
75	P-KPS	0.39	0.18	0.02	0.34	0.53	0.21	0.04	0.49
	BOP-KPS	86.93	49.93	6.42	71.30	131.95	85.27	11.01	100.70
	D-KPS	90.45	52.54	6.83	73.62	167.96	108.31	12.99	128.03
100	P-KPS	0.46	0.25	0.03	0.39	0.72	0.22	0.02	0.69
	BOP-KPS	50.60	29.80	4.62	41.01	72.93	47.17	6.17	55.62
	D-KPS	82.83	52.43	7.25	64.12	143.23	82.10	11.16	126.54
160	P-KPS	0.22	0.11	0.01	0.19	0.21	0.09	0.01	0.70
	BOP-KPS	90.93	53.92	6.87	73.22	171.01	115.04	13.71	126.53
	D-KPS	92.03	54.97	6.98	73.86	132.66	82.10	10.27	104.21

4.4. Measured 5G Throughput Quality Performance and Implication for Beyond-5G Wireless Networks

The maximum throughput quality obtained at closed measurement distances (25–160 m) from the assessed 5G NR broadband networks is between 1970 and 2350 Mbps. A closer look at the results shows that the maximum 5G throughput quality obtained at close distances from the gNodeB transmitter is quite below the envisioned and targeted integrity performance of 10–20 Gbps [50]. In order to ensure better throughput quality and excellent delivery of robust mobile connectivity in the present 5G NR networks and future wireless networks, the sub-6 GHz spectrum requires a lower site density spectrum. However, this provision comes at the critical expense of narrower bandwidths. Thus, massive MIMO optimization and higher-order modulation schemes are required to offer high-quality subscriber eMBB applications.

Another issue that should be addressed to achieve better throughput quality is the reduction in high penetration and propagation loss owing to higher spectrum deployment over 5G and beyond-5G wireless networks. The allocated spectrum bandwidth and type of service in 5G networks, such as the eMBB-enabled streaming, have an impact on the performance of the targeted throughput quality. During the design/deployment of future wireless systems in the 6G era, there is a need to evaluate how well the user equipment picks up at the login stage for optimization purposes.

The initial 5G deployment timing is controlled by the availability of 5G mobile devices, and this is often scarce owing to numerous key technical issues, such as the multi-band support of lower and upper-frequency bands, both of which can cause serious design challenges. In addition, the baseband processing results in enormous heating concerns, resulting from high power consumption during high-frequency band transmission. Thus, a more efficient power management technology is needed to solve the issues identified in 5G wireless networks.

Key emerging technologies that can be explored to meet the above efficient power management need and also provide a robust data throughput quality channel in the present 5G and the future 6G wireless communication systems are via the application of reconfigurable intelligent surfaces (RIS) [67,68]. The RIS engineering concept offers the opportunity to control the radio reliably signals en route to the transmitting stations and the receiving user equipment terminals in a proactive and goal-oriented way [67,69], which can boost the throughput data transmission capacity in a very dynamic way.

5. Conclusions

A detailed analysis of 5G throughput quality data obtained at different measurement distances (50, 75, 100, and 160 m) from the transmitter using the Gaussian mixture model is presented. The GMM clustering approach combines throughput quality levels with similar correlation sizes and constituent characteristics. Additionally, the work proposed and showed how the machine learning-based GPR predictive modeling can be enhanced when its kernel hyperparameters are rightly selected using the LBFGS with the KPS algorithm instead of the traditional Bayesian optimization, which is computationally expensive and does not always provide the optimal precision accuracy, particularly in the extrapolative analysis of large-scale dimensional data. Furthermore, the GPR–LBFGS with the KPS method was successfully exploited to mine the acquired throughput quality data through predictive analysis reliably. The proposed GPR model combined with the LBFGS with the KPS algorithm outperforms other methods because it iteratively provides better estimates of the kernel parameters, especially during optimization. The optimization involves conducting an enhanced line search of the kernel parameters that best minimizes the prediction errors. At separation distances of 25 m, 50 m, 75 m, 100 m, and 160 m, the proposed method attained 0.25, 0.16, 0.16, 0.22, and 0.43 RMSE accuracies, respectively, showing superior prediction accuracies compared to the preliminary methods. Lastly, the work identified and showed how throughput quality issues in 5G networks could be handled for optimal performance. Future work would extend the adopted robust GPR–LBFGS with the KPS method to conduct extrapolative analysis of other key 5G network parameters, such as signal strength and signal coverage quality assessment.

Author Contributions: The manuscript was written with the contributions of all authors. J.I. was responsible for the conceptualization of the topic; article gathering and sorting were carried out by J.I. and A.L.I.; manuscript writing, original drafting and formal analysis were carried out by J.I., A.L.I., S.O., D.-T.D. and C.-C.L.; writing of reviews and editing were carried out by A.L.I., S.O., D.-T.D. and C.-C.L.; and J.I. led the overall research activity. All authors have read and agreed to the published version of the manuscript.

Funding: The work of Agbotiname Lucky Imoize is supported in part by the Nigerian Petroleum Technology Development Fund (PTDF) and in part by the German Academic Exchange Service (DAAD) through the Nigerian-German Postgraduate Program under grant 57473408.

Institutional Review Board Statement: Not applicable.

Informed Consent Statement: Not applicable.

Data Availability Statement: The data that support the findings of this study are available from the corresponding author upon reasonable request.

Acknowledgments: The authors acknowledge the anonymous reviewers for the comments which help to improve the quality of the paper.

Conflicts of Interest: The authors declare no conflict of interest related to this work.

Abbreviations

5G	Fifth Generation
BOP	Bayesian Optimization
Gbps	Gigabits per second
GMM	Gaussian Mixture Model
GPR	Gaussian Process Regression
HSPA	High-speed Packet Access
KPS	Kernel Parameters Selection
LBFGS	Limited-memory Broyden–Fletcher–Goldfarb–Shanno
LTE	Long Term Evolution
MAPE	Mean Percentage Error

MAE	Mean Absolute Error
NR	New Radio
PDSCH	Physical Downlink Shared Channel
R	Coefficient of Correlation
RMSE	Root Mean Squared Errors
SEK	Squared Exponential Kernel
STD	Standard Deviation

References

1. Pang, J.; Wang, S.; Tang, Z.; Qin, Y.; Tao, X.; You, X.; Zhu, J. A new 5G radio evolution towards 5G-Advanced. *Sci. China Inf. Sci.* **2022**, *65*, 1–45. [CrossRef]
2. Lopez-Perez, D.; De Domenico, A.; Piovesan, N.; Xinli, G.; Bao, H.; Qitao, S.; Debbah, M. A Survey on 5G Radio Access Network Energy Efficiency: Massive MIMO, Lean Carrier Design, Sleep Modes, and Machine Learning. *IEEE Commun. Surv. Tutor.* **2022**, *24*, 653–697. [CrossRef]
3. Dahlman, E.; Parkvall, S.; Skold, J. *5G NR: The Next Generation Wireless Access Technology*; Academic Press: Cambridge, UK, 2020; ISBN 0128223219.
4. Imoize, A.L.; Adedeji, O.; Tandiya, N.; Shetty, S. 6G Enabled Smart Infrastructure for Sustainable Society: Opportunities, Challenges, and Research Roadmap. *Sensors* **2021**, *21*, 1709. [CrossRef]
5. Isabona, J.; Srivastava, V.M. Downlink massive MIMO systems: Achievable sum rates and energy efficiency perspective for future 5G systems. *Wirel. Pers. Commun.* **2017**, *96*, 2779–2796. [CrossRef]
6. Obakhena, H.I.; Imoize, A.L.; Anyasi, F.I.; Kavitha, K.V.N. Application of cell-free massive MIMO in 5G and beyond 5G wireless networks: A survey. *J. Eng. Appl. Sci.* **2021**, *68*, 1–41. [CrossRef]
7. Imoize, A.L.; Obakhena, H.I.; Anyasi, F.I.; Sur, S.N. A Review of Energy Efficiency and Power Control Schemes in Ultra-Dense Cell-Free Massive MIMO Systems for Sustainable 6G Wireless Communication. *Sustainability* **2022**, *14*, 11100. [CrossRef]
8. Imoize, A.L.; Tofade, S.O.; Ughegbe, G.U.; Anyasi, F.I.; Isabona, J. Updating analysis of key performance indicators of 4G LTE network with the prediction of missing values of critical network parameters based on experimental data from a dense urban environment. *Data Br.* **2022**, *42*, 108240. [CrossRef]
9. Simeone, O. A very brief introduction to machine learning with applications to communication systems. *IEEE Trans. Cogn. Commun. Netw.* **2018**, *4*, 648–664. [CrossRef]
10. Ma, S.; Zhu, Y.; Wang, G.; He, R. Machine learning aided channel estimation for ambient backscatter communication systems. In Proceedings of the 2018 IEEE International Conference on Communication Systems (ICCS), Chengdu, China, 19–21 December 2018; pp. 67–71.
11. Kaur, J.; Arif Khan, M.; Iftikhar, M.; Imran, M.; Haq, Q.E.U. Machine Learning Techniques for 5G and Beyond. *IEEE Access* **2021**, *9*, 23472–23488. [CrossRef]
12. Basha, S.M.; Rajput, D.S. Survey on evaluating the performance of machine learning algorithms: Past contributions and future roadmap. In *Deep Learning and Parallel Computing Environment for Bioengineering Systems*; Elsevier: Amsterdam, The Netherlands, 2019; pp. 153–164.
13. Isabona, J. Joint Statistical and Machine Learning Approach for Practical Data-Driven Assessment of User Throughput Quality in Microcellular Radio Networks. *Wirel. Pers. Commun.* **2021**, *119*, 1661–1680.
14. Divine, O.O.; Joseph, I. Application of Supervised Machine Learning Based on Gaussian Process Regression for Extrapolative Cell Availability Evaluation in Cellular Communication Systems. In Proceedings of the International Conference on Information and Communication Technology and Applications; 2020; pp. 130–144.
15. Ebhota, V.C.; Isabona, J.; Srivastava, V.M. 'Effect of Learning Rate on GRNN and MLP for the Prediction of Signal Power Loss in Microcell Sub-Urban Environment. *Int. J. Commun. Antenna Propag.* **2019**, *9*, 36–45. [CrossRef]
16. Singh, A.; Thakur, N.; Sharma, A. A review of supervised machine learning algorithms. In Proceedings of the 2016 3rd International Conference on Computing for Sustainable Global Development (INDIACom), New Delhi, India, 16–18 March 2016; pp. 1310–1315.
17. Ajani, T.S.; Imoize, A.L.; Atayero, A.A. An Overview of Machine Learning within Embedded and Mobile Devices—Optimizations and Applications. *Sensors* **2021**, *21*, 4412. [CrossRef]
18. Obahiagbon, K.; Isabona, J. Generalized Regression Neural Network: An Alternative Approach for Reliable Prognostic Analysis of Spatial Signal Power Loss in Cellular Broadband Networks. *Int. J. Adv. Res. Phys. Sci.* **2018**, *5*, 35–42.
19. Isabona, J.; Imoize, A.L. Optimal Kernel Selection Based on GPR for Adaptive Learning of Mean Throughput Rates in LTE Networks. *J. Technol. Adv.* **2021**, *1*, 1–21. [CrossRef]
20. Requeima, J.; Tebbutt, W.; Bruinsma, W.; Turner, R.E. The gaussian process autoregressive regression model (GPAR). In Proceedings of the The 22nd International Conference on Artificial Intelligence and Statistics, Naha, Japan, 16–18 April 2019; pp. 1860–1869.
21. Kopsiaftis, G.; Protopapadakis, E.; Voulodimos, A.; Doulamis, N.; Mantoglou, A. Gaussian process regression tuned by bayesian optimization for seawater intrusion prediction. *Comput. Intell. Neurosci.* **2019**, *2019*, 2859429. [CrossRef]

22. Morita, Y.; Rezaeiravesh, S.; Tabatabaei, N.; Vinuesa, R.; Fukagata, K.; Schlatter, P. Applying Bayesian optimization with Gaussian process regression to computational fluid dynamics problems. *J. Comput. Phys.* **2022**, *449*, 110788. [CrossRef]
23. Alali, Y.; Harrou, F.; Sun, Y. Optimized Gaussian Process Regression by Bayesian Optimization to Forecast COVID-19 Spread in India and Brazil: A Comparative Study. In Proceedings of the 2021 International Conference on ICT for Smart Society (ICISS), Bandung, Indonesia, 13 September 2021; pp. 1–6.
24. Isabona, J.; Ojuh, D.O. Machine Learning Based on Kernel Function Controlled Gaussian Process Regression Method for In-depth Extrapolative Analysis of Covid-19 Daily Cases Drift Rates. *Int. J. Math. Sci. Comput.* **2021**, *7*, 14–23. [CrossRef]
25. Lim, Y.-F.; Ng, C.K.; Vaitesswar, U.S.; Hippalgaonkar, K. Extrapolative Bayesian optimization with Gaussian process and neural network ensemble surrogate models. *Adv. Intell. Syst.* **2021**, *3*, 2100101. [CrossRef]
26. Yang, A.; Li, C.; Rana, S.; Gupta, S.; Venkatesh, S. Sparse Spectrum Gaussian Process for Bayesian Optimization. In Proceedings of the Pacific-Asia Conference on Knowledge Discovery and Data Mining, Virtual Event, 11–14 May 2021; pp. 257–268. [CrossRef]
27. Jafar, S.H. Financial Applications of Gaussian Processes and Bayesian Optimization. In *Bayesian Reasoning and Gaussian Processes for Machine Learning Applications*; Chapman and Hall/CRC: London, UK, 2022; pp. 111–122. ISBN 1003164269.
28. Rao, A.; Sarkar, B.; Narayanan, T. Gaussian Process Policy Optimization. *arXiv* **2020**, arXiv:2003.01074.
29. Berk, J.; Gupta, S.; Rana, S.; Venkatesh, S. Randomised gaussian process upper confidence bound for bayesian optimisation. *arXiv* **2020**, arXiv:2006.04296.
30. Benassi, R.; Bect, J.; Vazquez, E. Robust Gaussian process-based global optimization using a fully Bayesian expected improvement criterion. In *Learning and Intelligent Optimization*; Springer: Berlin, Germany, 2011; pp. 176–190.
31. Blum, M.; Riedmiller, M.A. Optimization of Gaussian process hyperparameters using Rprop. In *ESANN*; Citeseer: Philadelphia, PA, USA, 2013; pp. 339–344.
32. Kaedi, M.; Ghasem-Aghaee, N. Biasing Bayesian optimization algorithm using case based reasoning. *Knowl.-Based Syst.* **2011**, *24*, 1245–1253. [CrossRef]
33. Isabona, J.; Divine, O.O. A Gaussian Mixture Model with Firm Expectation-Maximization Algorithm for Effective Signal Power Coverage Estimation. In Proceedings of the International Conference on Information and Communication Technology and Applications, Minna, Nigeria, 24–27 November 2020; pp. 93–106.
34. Imoize, A.L.; Adegbite, O.D. Measurements-Based Performance Analysis of a 4G LTE Network in and Around Shopping Malls and Campus Environments in Lagos Nigeria. *Arid. Zone J. Eng. Technol. Environ.* **2018**, *14*, 208–225.
35. Imoize, A.L.; Oseni, A.I. Investigation and pathloss modeling of fourth generation long term evolution network along major highways in Lagos Nigeria. *Ife J. Sci.* **2019**, *21*, 39–60. [CrossRef]
36. Imoize, A.L.; Orolu, K.; Atayero, A.A.-A. Analysis of key performance indicators of a 4G LTE network based on experimental data obtained from a densely populated smart city. *Data Br.* **2020**, *29*, 1–17. [CrossRef] [PubMed]
37. Lee, D.; Lee, J. Machine learning and deep learning for throughput prediction. In Proceedings of the 2021 Twelfth International Conference on Ubiquitous and Future Networks (ICUFN), Jeju Island, Republic of Korea, 17–20 August 2021; pp. 452–454.
38. Li, L.; Ye, T. Research on throughput prediction of 5G network based on LSTM. *Intell. Converg. Netw.* **2022**, *3*, 217–227. [CrossRef]
39. Gao, Z. 5G traffic prediction based on deep learning. *Comput. Intell. Neurosci.* **2022**, *2022*, 3174530. [CrossRef]
40. Bakri, S.; Bouaziz, M.; Frangoudis, P.A.; Ksentini, A. Channel stability prediction to optimize signaling overhead in 5G networks using machine learning. In Proceedings of the ICC 2020–2020 IEEE International Conference on Communications (ICC), Dublin, Ireland, 7–11 June 2020; pp. 1–6.
41. Minovski, D.; Ogren, N.; Ahlund, C.; Mitra, K. Throughput prediction using machine learning in lte and 5g networks. *IEEE Trans. Mob. Comput.* **2021**, 1. [CrossRef]
42. Saputro, D.R.S.; Widyaningsih, P. Limited memory Broyden-Fletcher-Goldfarb-Shanno (L-BFGS) method for the parameter estimation on geographically weighted ordinal logistic regression model (GWOLR). In *AIP Conference Proceedings*; AIP Publishing LLC: Melville, NY, USA, 2017; Volume 1868, p. 40009.
43. Chen, T.; Ren, J. Bagging for Gaussian process regression. *Neurocomputing* **2009**, *72*, 1605–1610. [CrossRef]
44. Gbémou, S.; Eynard, J.; Thil, S.; Guillot, E.; Grieu, S. A comparative study of machine learning-based methods for global horizontal irradiance forecasting. *Energies* **2021**, *14*, 3192. [CrossRef]
45. Park, J.; Lechevalier, D.; Ak, R.; Ferguson, M.; Law, K.H.; Lee, Y.-T.T.; Rachuri, S. Gaussian Process Regression (GPR) Representation in Predictive Model Markup Language (PMML). *Smart Sustain. Manuf. Syst.* **2017**, *1*, 121–141. [CrossRef]
46. Nevin, J.W.; Vaquero-Caballero, F.J.; Ives, D.J.; Savory, S.J. Physics-informed Gaussian process regression for optical fiber communication systems. *J. Light. Technol.* **2021**, *39*, 6833–6844. [CrossRef]
47. Williams, C. *Gaussian Processes for Machine Learning. Inst. Adapt. Neural Comput.*; MIT Press: Cambridge, UK, 2007.
48. Berkenkamp, F.; Krause, A.; Schoellig, A.P. Bayesian optimization with safety constraints: Safe and automatic parameter tuning in robotics. *Mach. Learn.* **2021**, 1–35. [CrossRef]
49. Isabona, J.; Imoize, A.L.; Ojo, S.; Karunwi, O.; Kim, Y.; Lee, C.-C.; Li, C.-T. Development of a Multilayer Perceptron Neural Network for Optimal Predictive Modeling in Urban Microcellular Radio Environments. *Appl. Sci.* **2022**, *12*, 5713. [CrossRef]
50. Isabona, J.; Imoize, A.L.; Kim, Y. Machine Learning-Based Boosted Regression Ensemble Combined with Hyperparameter Tuning for Optimal Adaptive Learning. *Sensors* **2022**, *22*, 3776. [CrossRef]
51. Liu, D.C.; Nocedal, J. On the limited memory BFGS method for large scale optimization. *Math. Program.* **1989**, *45*, 503–528. [CrossRef]

52. Chen, W.; Wang, Z.; Zhou, J. Large-scale L-BFGS using MapReduce. *Adv. Neural Inf. Process. Syst.* **2014**, *4*, 27.
53. Gerber, F.; Furrer, R. optimParallel: An R package providing a parallel version of the L-BFGS-B optimization method. *R J.* **2019**, *11*, 352–358. [CrossRef]
54. Dovì, V.G.; Paladino, O.; Reverberi, A.P. Some remarks on the use of the inverse hessian matrix of the likelihood function in the estimation of statistical properties of parameters. *Appl. Math. Lett.* **1991**, *4*, 87–90. [CrossRef]
55. Lefkimmiatis, S.; Ward, J.P.; Unser, M. Hessian Schatten-norm regularization for linear inverse problems. *IEEE Trans. Image Process.* **2013**, *22*, 1873–1888. [CrossRef]
56. Isabona, J.; Srivastava, V.M. User-centric methodology for objective assessment of service quality in established Wireless Mobile Communication Networks. *Int. J. Commun. Antenna Propag.* **2017**, *7*, 26–30. [CrossRef]
57. Cox, C. *An Introduction to LTE: LTE, LTE-Advanced, SAE and 4G Mobile Communications*; John Wiley & Sons, Inc.: Hoboken, NJ, USA, 2012; ISBN 9781119942825.
58. Dahlman, E.; Parkvall, S.; Sköld, J. *4G: LTE/LTE-Advanced for Mobile Broadband*; Academic Press: Cambridge, MA, USA, 2013; ISBN 9780123854896.
59. Nguyen, S.L.H.; Haneda, K.; Järveläineny, J.; Karttuneny, A.; Putkonen, J. Large-Scale Parameters of Spatio-Temporal Short-Range Indoor Backhaul Channels at 140 GHz.2000. Available online: http://arxiv.org/abs/2009.13209 (accessed on 11 November 2022).
60. Shi, D.; Zhang, X.; Shi, L.; Vladimirescu, A.; Mazurczyk, W.; Cabaj, K.; Meunier, B.; Ali, K.; Cosmas, J.; Zhang, Y. On improving 5G internet of radio light security based on led fingerprint identification method. *Sensors* **2021**, *21*, 1515. [CrossRef] [PubMed]
61. Ajose, S.O.; Imoize, A.L. Propagation measurements and modelling at 1800 MHz in Lagos Nigeria. *Int. J. Wirel. Mob. Comput.* **2013**, *6*, 165–174. [CrossRef]
62. Imoize, A.L.; Ibhaze, A.E.; Nwosu, P.O.; Ajose, S.O. Determination of Best-fit Propagation Models for Pathloss Prediction of a 4G LTE Network in Suburban and Urban Areas of Lagos, Nigeria. *West Indian J. Eng.* **2019**, *41*, 13–21.
63. Tataria, H.; Haneda, K.; Molisch, A.F.; Shafi, M.; Tufvesson, F. Standardization of Propagation Models: 800 MHz to 100 GHz—A Historical Perspective.2000. Available online: http://arxiv.org/abs/2006.08491 (accessed on 20 September 2022).
64. Narayanan, A.; Ramadan, E.; Carpenter, J.; Liu, Q.; Liu, Y.; Qian, F.; Zhang, Z.-L. A first look at commercial 5G performance on smartphones. In Proceedings of the Web Conference 2020, Taipei, China, 20–24 April 2020; pp. 894–905.
65. Nakutis, Z.; Deksnys, V.; Jarusevicius, I.; Dambrauskas, V.; Cincikas, G.; Kriauceliunas, A. Round-trip delay estimation in opc ua server-client communication channel. *Elektron. Ir Elektrotechnika* **2016**, *22*, 80–84. [CrossRef]
66. Okakwu, I.K.; Oluwasogo, E.S.; Ibhaze, A.E.; Imoize, A.L. A comparative study of time series analysis for forecasting energy demand in Nigeria. *Niger. J. Technol.* **2019**, *38*, 465. [CrossRef]
67. Basharat, S.; Hassan, S.A.; Pervaiz, H.; Mahmood, A.; Ding, Z.; Gidlund, M. Reconfigurable intelligent surfaces: Potentials, applications, and challenges for 6G wireless networks. *IEEE Wirel. Commun.* **2021**, *28*, 184–191. [CrossRef]
68. Sharma, T.; Chehri, A.; Fortier, P. Reconfigurable Intelligent Surfaces for 5G and beyond Wireless Communications: A Comprehensive Survey. *Energies* **2021**, *14*, 8219. [CrossRef]
69. Kumaravelu, V.B.; Imoize, A.L.; Soria, F.R.C.; Velmurugan, P.G.S.; Thiruvengadam, S.J.; Murugadass, A.; Gudla, V.V. Outage Probability Analysis and Transmit Power Optimization for Blind-Reconfigurable Intelligent Surface-Assisted Non-Orthogonal Multiple Access Uplink. *Sustainability* **2022**, *14*, 13188. [CrossRef]

Disclaimer/Publisher's Note: The statements, opinions and data contained in all publications are solely those of the individual author(s) and contributor(s) and not of MDPI and/or the editor(s). MDPI and/or the editor(s) disclaim responsibility for any injury to people or property resulting from any ideas, methods, instructions or products referred to in the content.